American Scientific Research Journal for Engineering, Technology, and Sciences (ASRJETS)
ISSN (Print) 2313-4410, ISSN (Online) 2313-4402
© Global Society of Scientific Research and Researchers
http://asrjetsjournal.org/

Fuselage Surface Pressure Effects due to Wing Interferences

Umran Abdul Rahman[a]*, Faizal Mustapha[b]

[a]*Dr, Engineering & Maintenance Department, Malaysia Airlines Berhad, KLIA Sepang, 64000 Malaysia*
[b]*Professor, Engineering Faculty, University Putra Malaysia, Serdang, 43400 Malaysia*
[a]*Email: umran.abdulrahman@malaysiaairlines.com*
[b]*Email: faizalms@upm.edu.my*

Abstract

A streamlined fuselage with a rounded cross-sectional area attached with Onera M6 wing was tested using a compressible RANS CFD. Coupled with k-omega SST turbulent model, the craft was tested at 0.8359 Mach which corresponds to 11.72 x 10^6 Reynolds number. At 3.06˚ wing incidence angle, this simulation is to highlight the fuselage surface pressure variations at the interference region for preliminary aircraft design consideration. By keeping up closely with the physically tested wing through wind tunnel, the results of this simulation can be justified.

Keywords: RANS; Compressible; Onera M6; Interference; Design.

1. Introduction

Wing to fuselage interference has been the subject of research from the early days of aviation history. Many of the discussion primarily focuses on the net effect of the total aerodynamic performance of the aircraft or any other 'craft'. The craft here can be either submarine, blimp, missiles and also rockets. These researches can be referred but not exhaustively to [1-5] & [6].In this paper however, we would like to channel the discussion towards the actual effect on the component itself (fuselage to be precise) due to the aerodynamic interferences that occurred as the machine moves through the air. Although the model used is fictitious in nature, however, it stems out from the actual occurrences involving commercial jets of which the author has the firsthand experience in investigating the issue.

---

* Corresponding author.

2. Background

The demand for a faster flight time in today's business world pushes aircraft manufacturers to design the large commercial jets ever closer to unity Mach number in terms of its cruising velocity. Passing this however, the economic viability is very much a concern [7]. For a quick reference, B747-400 have a cruising Mach number of 0.855 [8] while Airbus A380 is at 0.85 [9]. Although these numbers do not passed unity, nevertheless during cruise, expectedly at some region within the aircraft, the airflow may cross over and when it does, consequentially so does the increase on the effects caused by the surface pressure variations. It will be best to convey these effects through the use of the actual affected aircraft which was investigated, however, since it involves proprietary information and there were no public accessible references, a build up model was used instead.

To simulate the effect, a steady state Reynolds-average Navier-Stokes (RANS) CFD simulation was conducted using the OpenFOAM® CFD package while k-omega SST [10] turbulent model was used to close the RANS equations. For the validation process, Onera M6 wing was used where the experimental results were readily available for direct comparisons [11]. The chosen solver for this simulation is the steady-state compressible solver, rhoSimpleFoam, where, it stems out from SIMPLE (Semi-Implicit Method for Pressure Linked Equations) architecture developed by ref [12] of which, ref [13] provides more in-depth practical application of the methods involved.

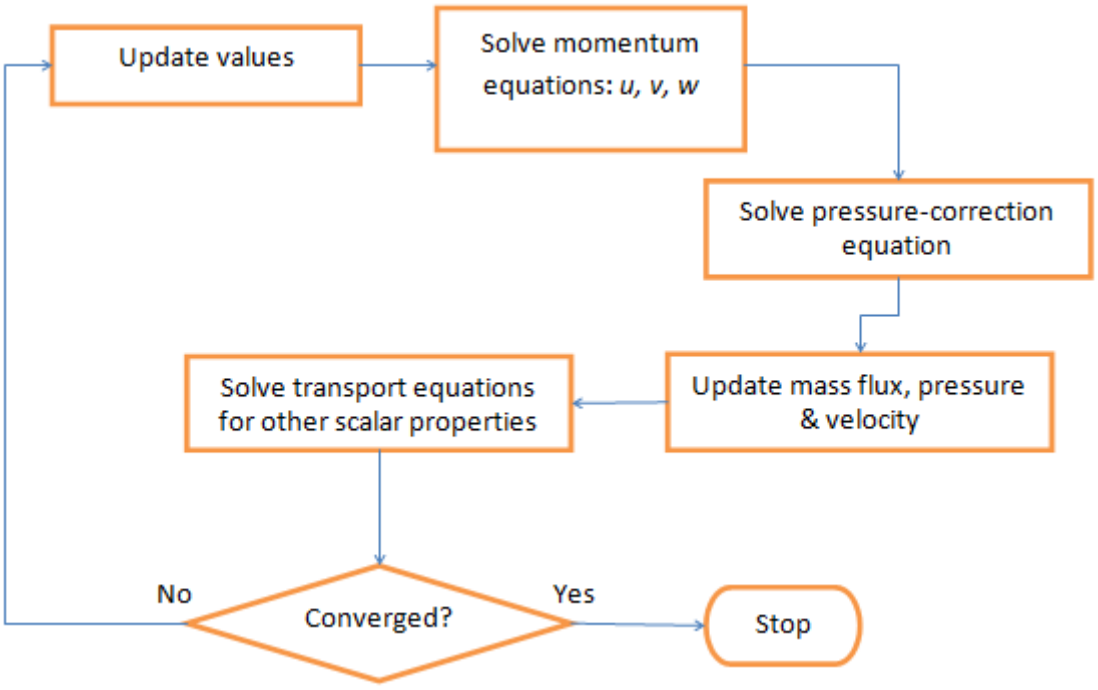

Figure 1: SIMPLE workflow

3. Modeling & Meshing

Referring to Figure 2, a half missile shaped fuselage was employed as the wing carrier. The wing 40% chord

was placed at the middle of this 12-meter-long body. The wing attachment is direct i.e. without any wing to fuselage fillet, though, to close the mating between the flat root airfoil with the rounded fuselage, the wing skin being extended accordingly so as there are no gaps in generating the STL file for the model.

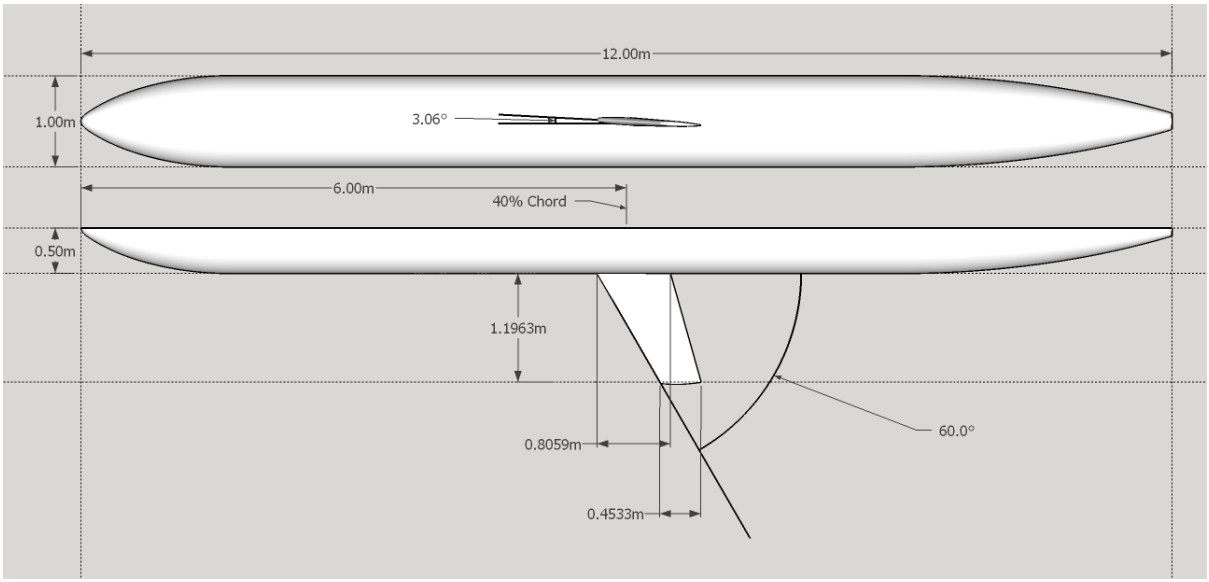

Figure 2: Onera M6 wing on simulation fuselage body

With 0.5 m fuselage radius, the wing airfoil and incident angle, root chord, tip chord, swept back angle and wing span (not included half fuselage thickness) follows almost exactly as per [14] except for some minor rounding off errors.

The calculation domain comprises of a rectangular box measuring 40 x 40 x 100 m while the model was placed at 20 m from the inlet (Figure 3 refers).

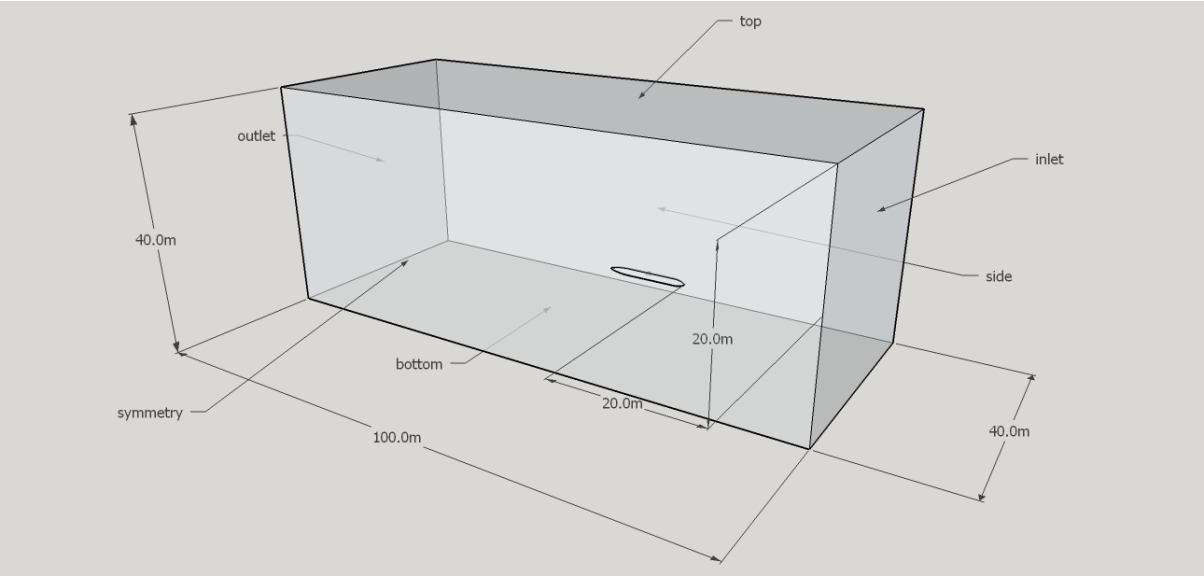

Figure 3: Calculation domain

Meshing of the domain was done using blockMesh while snappyHexMesh was used to refine while adding 2 layered meshes on the model surfaces (both meshing tools were provided for in OpenFOAM® packages). From the initial 1 m block cell at the edges of the domain, with 9 levels of refinement, the surface mesh sizes reduced to 1.95 x 10^{-3} m sides resulting with the final count of 6,358,781 cells.

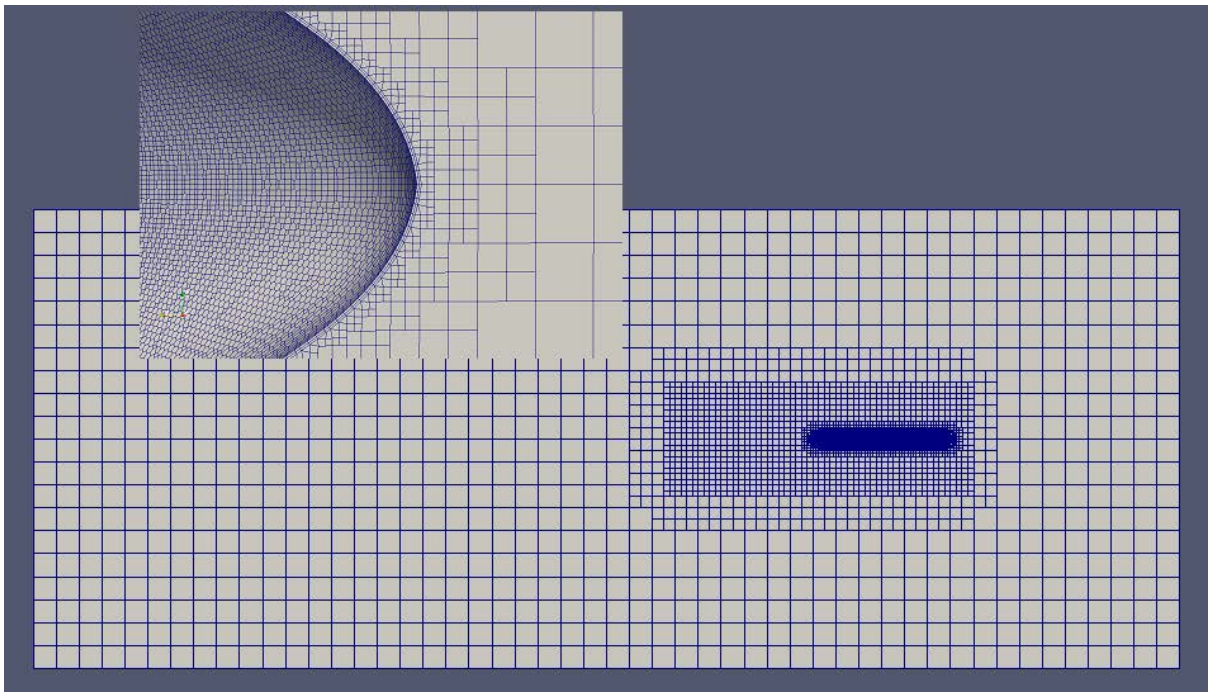

Figure 4: Overall mesh and the zoomed in layers detail

4. Flow Parameters

As with the actual Onera M6 wing, the flow parameters were fixed as below,

- Velocity: 0.8395 Mach (294.23 m/s).
- Temperature: 305.7 Kelvin.
- Pressure: 101325 N/m^2 (Standard Sea Level pressure).

By taking only the wing MAC (Mean Aerodynamic Chord) as the primary wetted length and standard sea level dynamic air viscosity, these parameters correspond to 11.72 x 10^6 Reynolds number of which the Onera M6 wind tunnel testing results were based on. Apart from these, additional initial values of k and omega at the boundaries were estimated based from ref [15].

5. Running the Simulation

In the initial phase, upwind discretization was used for all divergence schemes ($\nabla.\phi$ – theta here represent any of the transport variables) as it is more stable and converge rather easily. At 1629^{th} iteration, the simulation converged i.e. all parameter residuals dropped below 1 x 10^{-6}. To improve the precision level of the obtained

results [16], the divergence schemes were replaced with limited linear schemes (a combination of first order upwind at rapidly changing gradients and a second order central differencing scheme elsewhere). Under this scheme, the simulation was allowed to run up to 4000 iterations (from 1629), at which the solved variables change very little at each iteration thereafter.

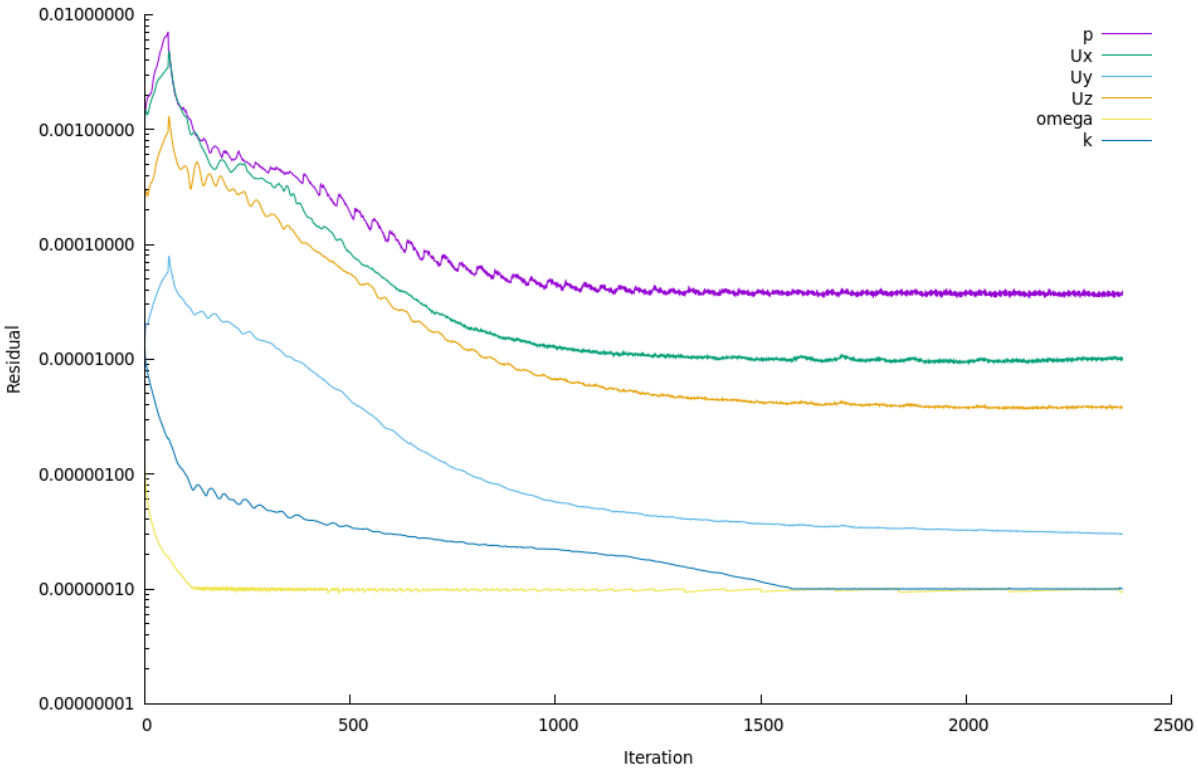

Figure 5: Second Phase Residuals

6. Results & Discussions

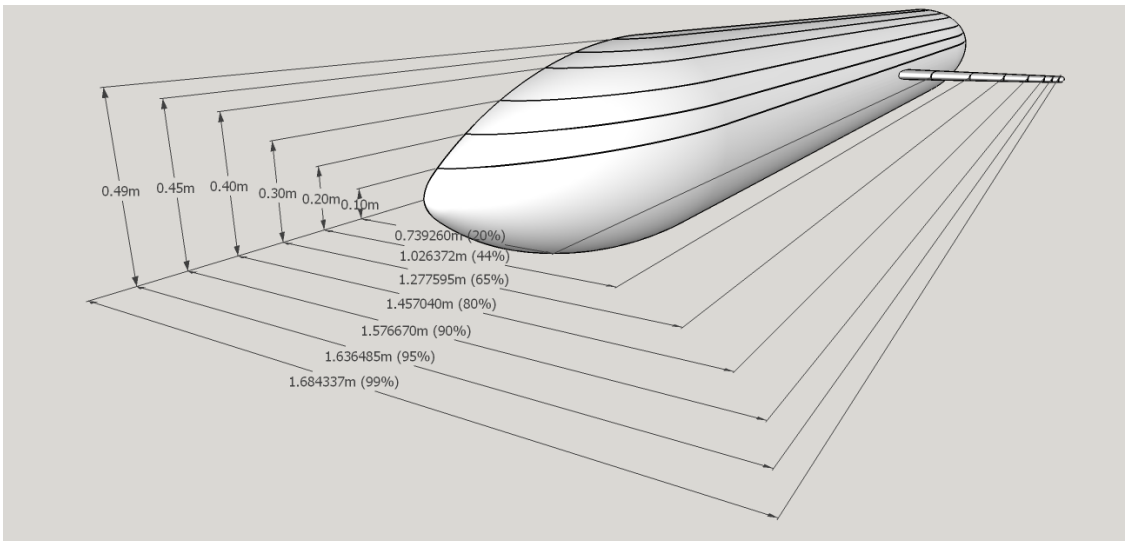

Figure 6: Sampling locations

For control purposes, surface pressure sampling was done for the wing itself where the sampling stations were located at various percentage of the wing span following the obtained data from the wind tunnel experiment.

Expectedly some differences will be there as the appearance of the fuselage, however, certain quantum of comparability will help in deducing the validity of the obtained results.

As shown on Figure 6, apart from those wing sampling stations, on the fuselage itself, vertical sampling stations being located in the increment of 0.1 m from fuselage datum except for the top 2 stations which is 0.05 and 0.04 m apart respectively.

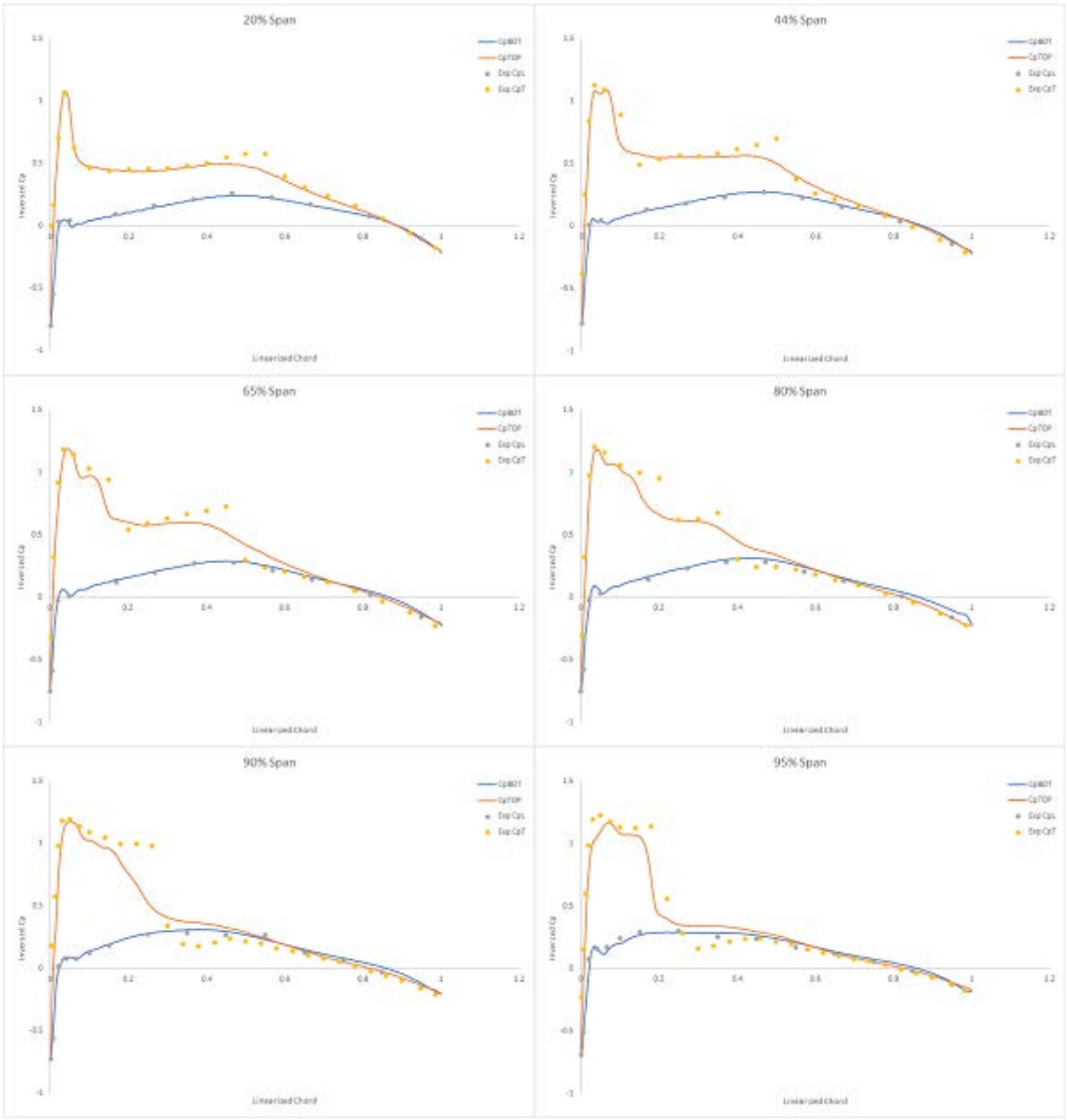

Figure 7: 20, 44, 65, 80, 90 & 95% wing span samplings

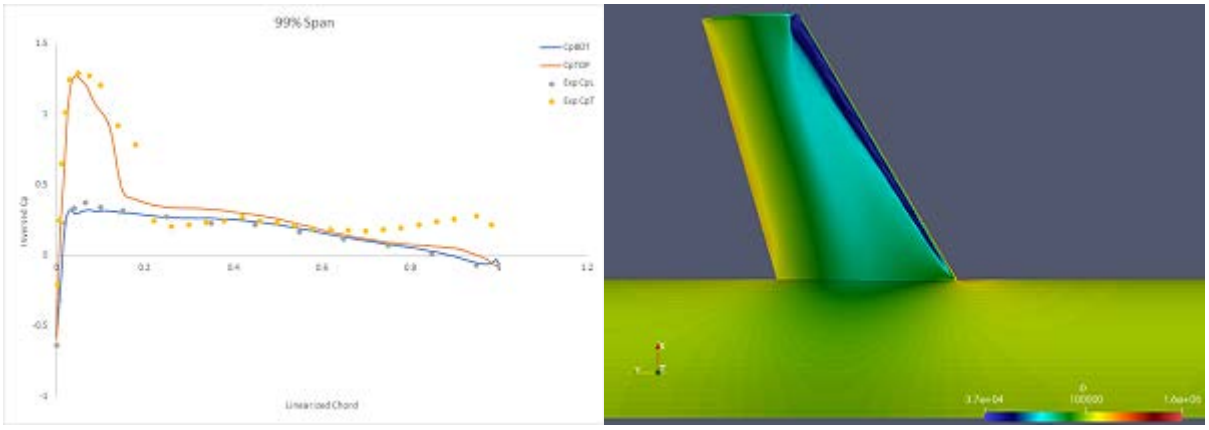

Figure 8: 99% wing span samplings & top wing surface pressure gradients

Referring to Figure 7 & 8, although the bottom wing pressure coefficients follow closely with the experimental results, the same couldn't be said about the top wing. The second weak shock (appeared on the experimental results at roughly mid chord area along the span) apparently becoming bland and this can be explained via inspecting Figure 9 below.

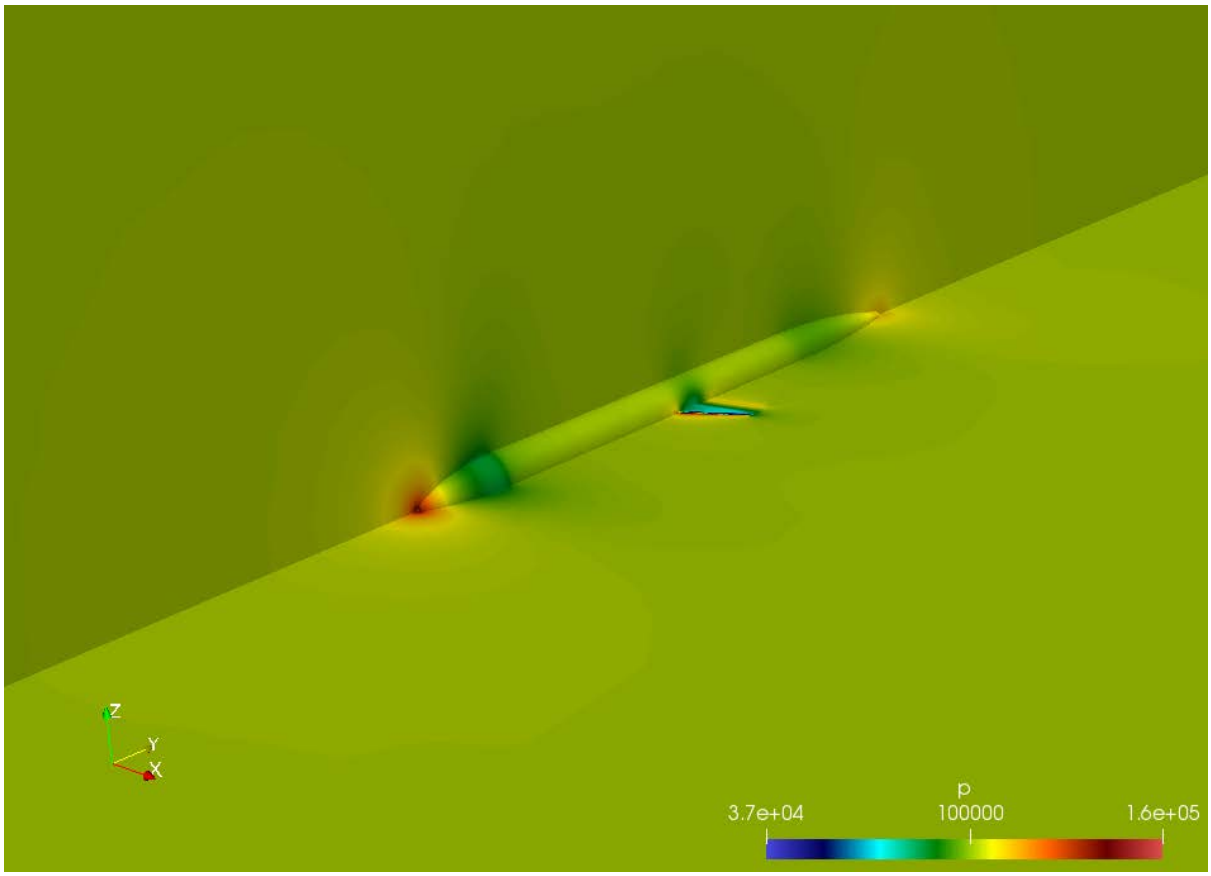

Figure 9: Pressure Bubble

Prior to reaching the wing, the airflow must pass through the pressure bubble formed by the appearance of the fuselage and this dampens the effect when compared to a direct flow across the wing by itself and thus weaken

the shocks. Nonetheless, the typical appearance of the λ shaped pressure gradients on the top of the wing is another indication that this simulation is pointing to the right direction (refer to Figure 8 right). Based on this observation and the comparative studies of the obtained wing stations data, the validity of this simulation can be verified and thus, the obtained samplings from the fuselage can be used with higher degree of confidence.

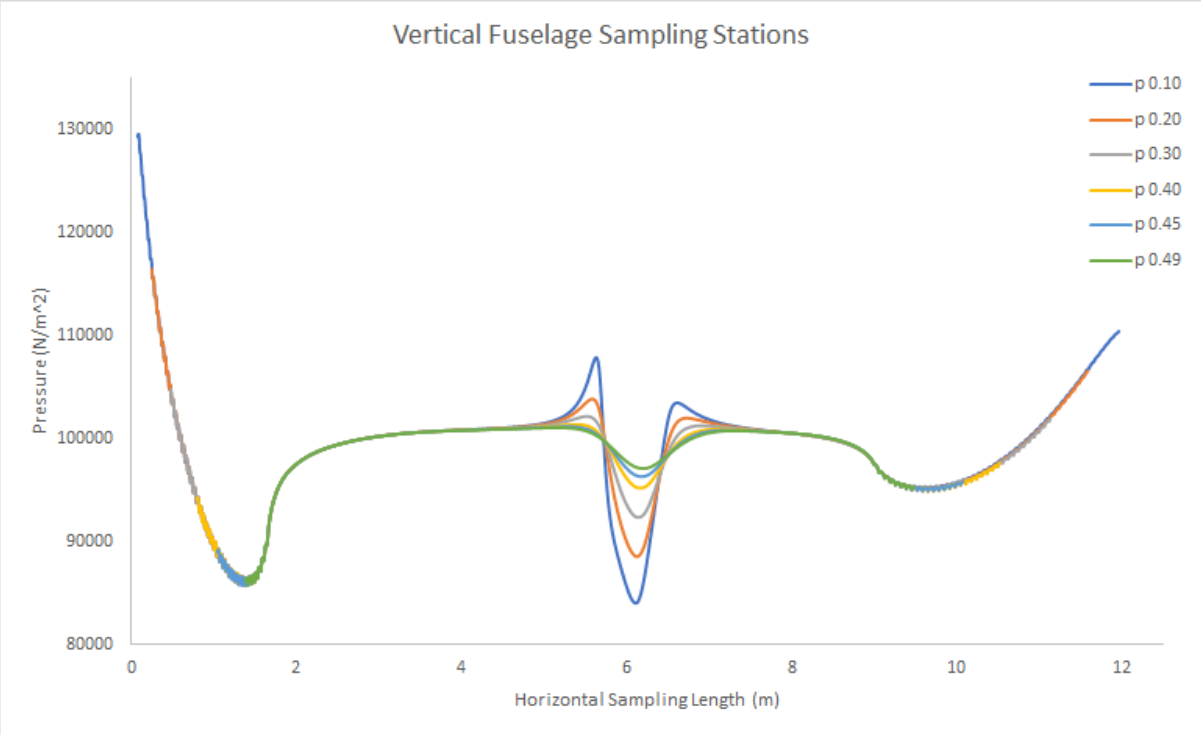

Figure 10: Fuselage surface pressure samplings

An interesting fuselage surface pressure pattern can be observed on Figure 10. Except at the mid fuselage region, consistent overlay of pressure values on top of each other can be viewed even though the sampling locations were distanced significantly away from each other. The different here is only limited to the sampling line length. This shows that at any location along the longitudinal direction, disregards their elevation height, same surface pressure should appear as the airflow parameters are the same longitudinally due to symmetrical in nature. This is only true where there were no interferences from the wing while the effects of gravity on the air particles were neglected. Along the fuselage, between 5 to about 7.5 m, the fuselage surface suffers some pressure variations where the highest disturbance located nearest to the wing joint. Although the variations becoming weaker as sampling height increases, nonetheless, it is still apparent all the way to the roof of the fuselage. There are 2 significant considerations with regard to these results,

i. At this region, apart from the cyclic skin stresses due to pressurization (for commercial passenger transport aircraft), additional cyclic stresses due to external surface variations needed to be factored in to determine the airframe life.
ii. The moment loading effect due to surface pressure variation needed to be considered prior to any placement of exterior substructure at this sensitive region.

For item i, the low exterior pressure region will cause additional strain to the fuselage skin which was already under internal pressure at cruising height. This will induce additional fatigue thus reducing the service life.

On item ii, as an example, consider a placement of a rectangular flat SATCOM (Satellite Communication) antenna at the top of the fuselage just aft of the maximum pressure dip, refer Figure 10). Longitudinally, this antenna will experience a relatively low pressure at the forward edge while a much higher surface pressure at the rear. These differences will cause an unaccounted moment loading on the surface of this antenna which will have the tendency to lift the frontal edges and subsequently ripping it off from the skin.

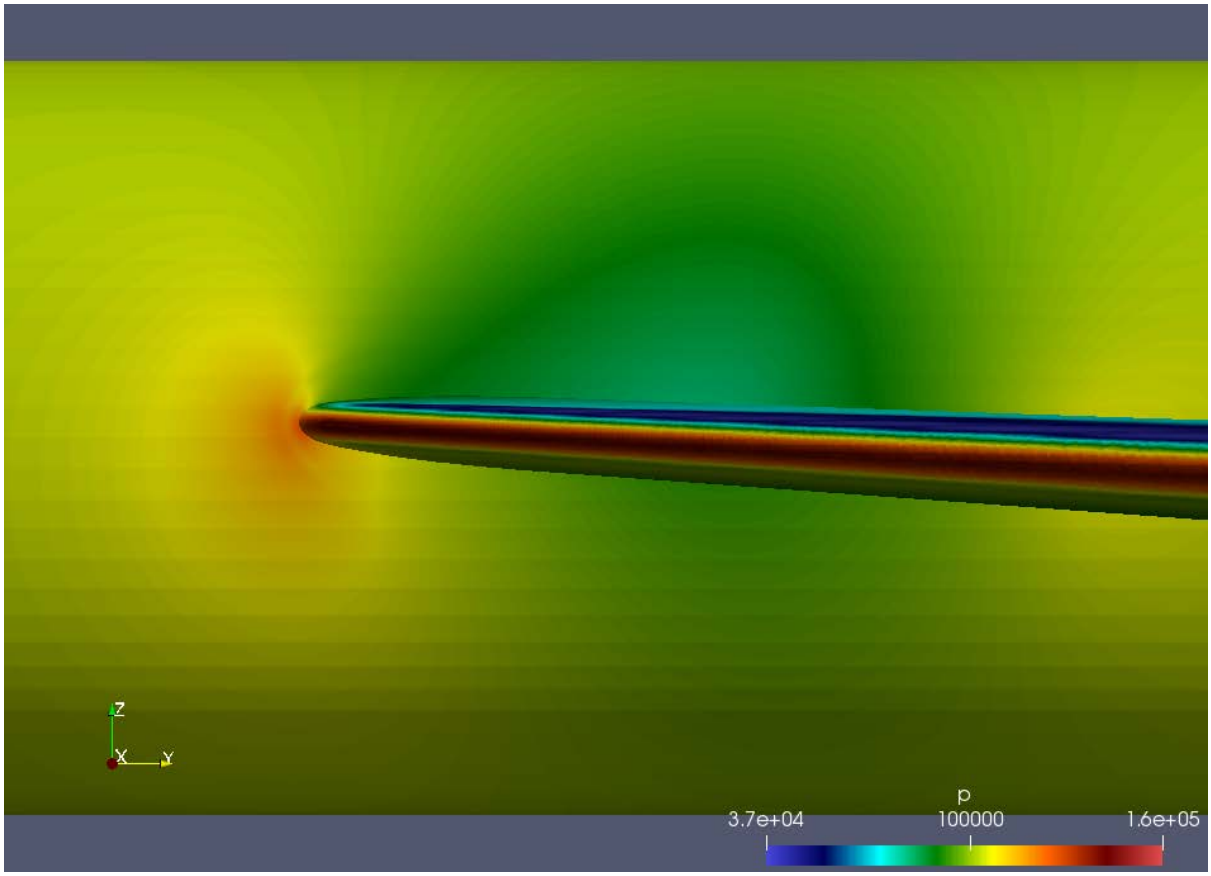

Figure 11: Intersection region fuselage surface pressure variation

7. Conclusions

Apart from the obvious effect on aerodynamic performance of an aircraft due to interference flow, this simulation result shows that the resulting pressure variation on fuselage surfaces needed to be considered during the design stage of an aircraft.

Although the fuselage model in use was just a drafted model without any direct reference to any physical model, the comparative results on the wing does however, provide the justifications on the obtained data from this simulation.

8. Recommendation

There are 3 distinct phases of aircraft design philosophy, namely, conceptual, preliminary and finally detail design. Typically, during preliminary stage, the drafted conceptual design is locked down and more detail load studies will be conducted. For a more recent designs, CFD analysis play an important role in determining the overall performance and the expected aerodynamic loadings. Here is where an interjection requires where the scope of the intersection region must be properly identified (based on the expected flight envelope) and any would be placement of structure or sub-structure within this region must be thoroughly studied as part of the load analysis.

Having experienced the real-world issues on this subject, costly modification and rework may be required if this phenomenon was over sighted.

Acknowledgements

The Author would like to thank the Board Members of School of Graduate Studies, University Putra Malaysia (UPM). Thanks also to D.Eng program advisors Dr. Mohamed Thariq and Dr. Azmin Shakrine for the guidances given in preparing this paper. To Prof. Dr. Abdul Aziz and Prof. Dr. Nik Abdullah from University Malaysia Pahang (UMP), thanks for the interest in Author's work. Special thanks to The Ministry of Education, Malaysia for the granted scholarship under MyBrain15 program.

References

[1] MAUGHMER, M., Hallman, D., Ruszkowski, R., Chappel, G., & Waitz, I. (1989). Experimental investigation of wing/fuselage integration geometries. Journal of Aircraft, 26(8), 705-711.

[2] Shankar, V., & Malmuth, N. (1981). Computational and Simplified Analytical Treatment of Transonic Wing/Fuselage/Pylon/Store Interactions. Journal of Aircraft, 18(8), 631-637.

[3] Caughey, D. A., & Jameson, A. (1979). Numerical calculation of transonic potential flow about wing-body combinations. AIAA Journal, 17(2), 175-181.

[4] Boppe, C. W. (1980). Transonic flow field analysis for wing-fuselage configurations.

[5] Ross, J., CORSIGLIA, V., & VOGEL, J. (1981, August). Full-scale wind-tunnel study of wing-fuselage interaction and comparison with paneling method. In Aircraft Systems and Technology Conference (p. 1666).

[6] Chigier, N. A., & Corsiglia, V. R. (1972). Wind-tunnel studies of wing wake turbulence. Journal of Aircraft, 9(12), 820-825.

[7] Liebhardt, B., & Lütjens, K. (2011). An Analysis of the Market Environment for Supersonic Business Jets. German Aerospace Center (DLR)–Air Transportation Systems, Hamburg.

[8] https://www.boeing.com/resources/boeingdotcom/company/about_bca/startup/pdf/historical/747-400-passenger.pdf

[9] https://www.airbus.com/content/dam/corporate-topics/publications/backgrounders/Backgrounder-Airbus-Commercial-Aircraft-A380-Facts-and-Figures-EN.pdf

[10] Menter, F. R. (1994). Two-equation eddy-viscosity turbulence models for engineering applications. AIAA journal, 32(8), 1598-1605.

[11] Rahman, U. A., & Mustapha, F. (2015, February). Validations of OpenFoam Steady State Compressible Solver Rhosimplefoam. In International Conference on Mechanical and Industrial Engineering.

[12] Patankar, S. V. (1980). Numerical Heat Transfer and Fluid Flow Taylor & Francis. New York.

[13] Fergizer, J. H., & Peric, M. Computational Methods for Fluid Dynamics. 2002.

[14] Schmitt, V. and F. Charpin, "Pressure Distributions on the ONERA-M6-Wing at Transonic Mach Numbers," Experimental Data Base for Computer Program Assessment. Report of the Fluid Dynamics Panel Working Group 04, AGARD AR 138, May 1979.

[15] http://www.cfd-online.com/Wiki/Turbulence_free-stream_boundary_conditions - 18/07/2013.

[16] Jasak, H. (1996). Error analysis and estimation for the finite volume method with applications to fluid flows.